Aug 14th, 12:00 AM - Aug 15th, 12:00 AM

Flexural Behavior and Design of the New Built-up LiteSteel Beams

Sivapathasunderam Jeyaragan

Mahen Mahendran

Nineteenth International Specialty Conference on Cold-Formed Steel Structures
St. Louis, Missouri, U.S.A, October 14 & 15 2008

Flexural Behavior and Design of the New Built-up LiteSteel Beams

Sivapathasunderam Jeyaragan[1] and Mahen Mahendran[2]

Abstract

A new cold-formed steel beam, known as the LiteSteel Beam (LSB), has the potential to transform the low-rise building industry. The new beam is effectively a channel section with two rectangular hollow flanges and a slender web, and is manufactured using a simultaneous cold-forming and electric resistance welding process. Built-up LSB sections are expected to improve their flexural capacity and to increase their applications. They are also likely to mitigate the detrimental effects of lateral distortional buckling observed with single LSB members of intermediate spans. However, the behaviour of built-up beams is not well understood. Currently available design rules based on longitudinal connection spacing limits and doubling the capacity of single members were found to be inadequate. Therefore a research project based on both experimental and advanced numerical studies was undertaken to investigate the flexural behaviour of back to back LSBs with various longitudinal connection spacings under a uniform moment. This paper presents the details of the experimental and numerical studies and the results.

1. Introduction

LiteSteel Beam (LSB) is a new cold-formed steel beam produced by Australian Tube Mill (ATM) and marketed by LiteSteel Technologies (LST). The new beam is effectively a channel section with two rectangular hollow flanges and a slender web, and is manufactured using a simultaneous cold-forming and electric resistance welding process. It has a unique shape with superior torsional strength properties and provides a very high strength to weight ratio. Figure 1

[1] PhD Student & [2] Professor, School of Urban Development, Queensland University of Technology, Brisbane, QLD 4000, Australia

illustrates the LSB cross-section and its typical use. LST is promoting the LSBs as floor bearers in residential construction, replacing hot-rolled beams (Fig. 2).

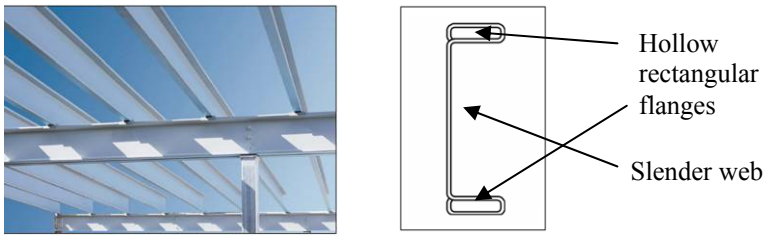

Figure 1: LiteSteel beam (LST, 2005)

Built-up LSB sections are expected to improve their flexural capacity and to expand their usage to long span applications. They can be fabricated using the traditional back to back configuration as shown in Figure 2 and can produce more than double the bending capacity of single LSBs. Mahaarachchi and Mahendran's (2005a) research on single LSB sections found the LSBs to be susceptible to Lateral Distortional Buckling (LDB). The back to back built-up LSB is likely to mitigate LDB effects to some extent by proving additional rigidity to the weakest element of the section, namely the web. However, the behaviour of built-up beams is not well understood and the current design rules are found to be inadequate in some applications. This paper presents the details of an investigation using experimental and numerical studies on back to back built-up LSB sections, the calibration of finite element models and the results.

Figure 2: Back to back built-up LSBs (LST, 2005)

2. Current Design Rules

AS/NZS 4600 (SA, 2005) gives limited guidance in relation to the fastener arrangements required to ensure full compatibility between the sections. Clause 4.1.1 specifies that the maximum longitudinal spacing (s_{max}) of welds or other connectors joining two channels to form an I-section is as follows:

$$s_{\max.} = \frac{l}{6} \leq \frac{2 s_g N^*}{mq} \tag{1}$$

where l = span of beam, N^* = design strength of connectors in tension, q = intensity of the design action on the beam, s_g = vertical distance between two rows of connections nearest to the top and bottom flange, m = distance from the shear centre of one channel to the mid-plane of its web.

It also gives details for determining the design load (q) and unequal connection spacing. The American cold-formed steel code (AISI, 2001) provides identical or very similar guidelines for cold-formed built-up beams as for AS/NZS 4600.

BS 5950 Part 5 (BSI, 1998) specifies the required strength of connectors at preventing fastener failures, which is similar to AS/NZS 4600 (SA, 2005) whereas the design rules given for preventing excessive distortion between connectors differ and are given as follows:

1) The beam length is divided into at least three equal parts: ie. $s_{max} \leq \frac{l}{3}$
2) $s \leq 50\ r_{cy}$ where s = the longitudinal spacing of connections, r_{cy} = the minimum radius of gyration of one channel

BS 5950 Part 5 (BSI, 1998) also specifies effective lengths for compound sections in terms of fastener spacing (Clause 5.6.3). In compound sections composed of two channels back to back designed as a single integral member and connected in accordance with Clause 8.6, the effective slenderness of the compound beam (L_E/r_y) should be calculated as follows:

$$\frac{L_E}{r_y} = \sqrt{\left(\frac{L_E}{r_I}\right)^2 + \left(\frac{s}{r_{cy}}\right)^2} \quad > 1.4\ \mathrm{s/r_{cy}} \tag{2}$$

Where

L_E - the effective length of the compound member, r_y - the radius of gyration of the compound section about the axis parallel to the webs allowing for the two elements acting as a single integral member, r_I - the radius of gyration of the compound section about the axis parallel to the webs based on normal geometric properties, s - the longitudinal spacing between adjacent fasteners or welds connecting the two sections, r_{cy} - the min. radius of gyration of one channel. The local slenderness of an individual channel section, s/r_{cy}, should not exceed 50.

3. Experimental Study

3.1 Test specimen and test program

Based on a numerical study, Compact, Non-compact and Slender LSB sections were chosen. Test span selected was 3.5 m based on current test rig capacity and the practical range of 12 to 24 times of section depth (d). Connector spacings (CS) selected for the specimens are the minimum spacing of span/6 as specified in AS/NZS 4600, span/4, span/3, span/2 and span/1, ie. no connections between the two end supports. For comparison purposes, single LSBs were also tested. Details of the test specimens are reported in Table 1.

3.2 Test set-up and procedure

The lateral buckling tests were carried out using an overhang loading method in which a uniform moment was provided throughout the entire span (L). Attempts were taken to reduce the level of warping restraint. Although shorter overhangs induce less restraint, they may induce shear or local buckling failure at the supports due to higher load requirements. An appropriate overhang length of 0.75 m (X) was chosen based on preliminary finite element analyses to avoid any premature failures. The experimental arrangement of built-up LSB beams used in this research is shown in Figure 3. The test rig used by Mahaarachchi and Mahendran (2005a) for single LSB sections was modified for the built-up LSB sections. It consists of a support system and a loading system, attached to an external frame structure (Figure 4a).

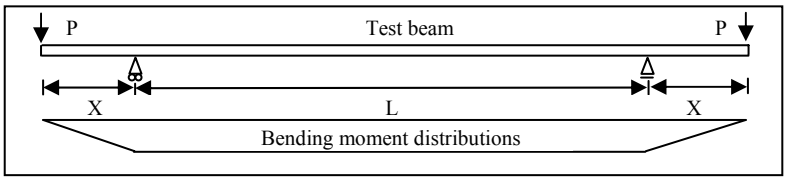

Figure 3: Overhang loading method

The support systems were designed to ensure that the test beams were simply supported in-plane and out-plane (Figure 4b). The support conditions restrained in-plane vertical deflection, out-of-plane deflections and twisting, but allowed major and minor axis rotations. One of the supports was designed as a roller. In addition, two brackets were designed to be located at the end support systems to hold back to back LSBs without any gap. Loading arms were specially designed to apply the loads through the shear centre. The loading system was designed to

prevent any restraint to the displacement and rotations of the test beam using a special wheel system. The loads were applied at the end of each overhang under displacement control method using hydraulic rams.

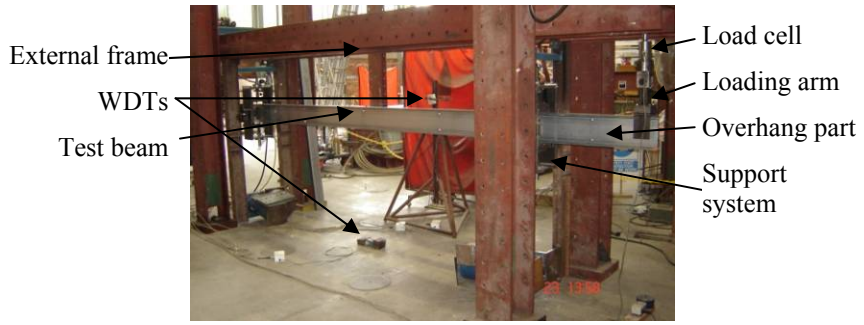

(a) Overall view of test rig

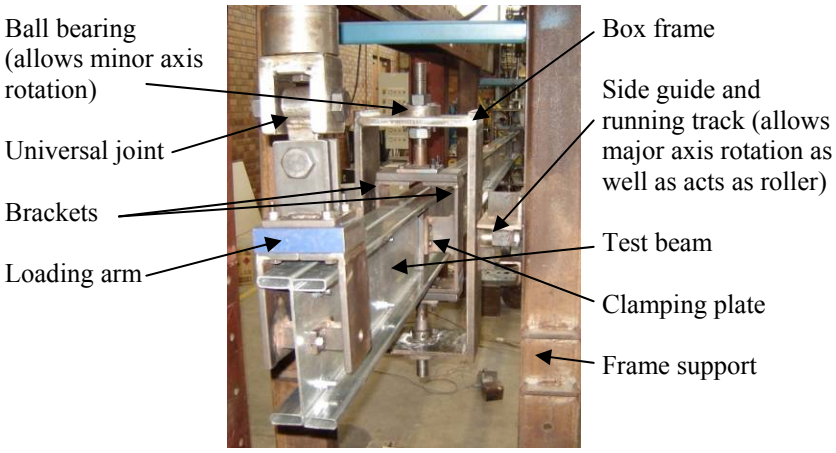

(b) Support system

Figure 4: Test set-up

The loads were applied to the test beam until its failure while recording the measurements of the applied load, beam deformations and strains. The in-plane and out of plane deflections of top and bottom flanges at midspan, and the vertical deflection under each loading point of the overhang deformations were measured using wire potentiometer type displacement transducers (WDT). Longitudinal strains were also recorded at midspan using strain gauges.

4. Experimental Results

Experimental responses of built-up beams were evaluated based on four important parameters, the moment capacity, bending deformations, failure mode and the flange separation. More details are given in Jeyaragan and Mahendran (2008a). Table 1 presents the test results and the three important parameters.

Table 1: Experimental test results and identified parameters

Test No	Specimens $d \times b_f \times t$	Span (mm)	Type	s (mm)	M_u (kNm)	δ_v (mm)	Failure Mode
1	200×45×1.6 LSB	3500	B	3500	17.15	14.2	LDB
2	200×45×1.6 LSB	3500	B	1750	17.00	17.6	LDB
3	200×45×1.6 LSB	3500	B	1167	21.06	12.6	LDB
4	200×45×1.6 LSB	3500	B	875	17.93	15.7	LDB
5	200×45×1.6 LSB	3500	B	583	20.64	14.4	LDB
6	150×45×1.6 LSB	3500	B	3500	17.43	30.8	LDB
7	150×45×1.6 LSB	3500	B	1750	17.28	30.8	LDB
8	150×45×1.6 LSB	3500	B	1167	17.71	33.2	LDB
9	150×45×1.6 LSB	3500	B	875	16.68	30.4	LDB
10	150×45×1.6 LSB	3500	B	583	19.55	35.1	LDB
11	125×45×2.0 LSB	3500	B	1167	20.63	55.8	LDB
12	125×45×2.0 LSB	3500	B	583	19.84	54.4	LDB
13	150×45×1.6 LSB	3500	S	N/A	6.52	39.3	LDB
14	200×45×1.6 LSB	3500	S	N/A	7.33	13.0	LDB

Note: d – Overall depth, b_f – Flange width, t – Thickness, s – Connector spacing, M_u – Ult. Moment, δ_v – Vertical displacement at midspan, LDB – Lateral Distortional Buckling, B – back to back built-up LSB, S – single LSB.

4.1 Influence of connector spacing and comparison with single LSBs

The moment capacities of built-up 200×45×1.6 LSBs range from 17.00 kNm for connector spacing of span/2 to 21.06 kNm for connector spacing of span/3 whereas the moment capacity of corresponding single LSB is 7.33 kNm. For 150×45×1.6 LSB, the moment capacities varied from 17.28 kNm for connector spacing of span/2 to 19.55 kNm for connector spacing of span/6 while the moment capacity of corresponding single LSB is 6.52 kNm. Hence in general, test results show that the moment capacity of built-up LSBs is influenced by the connector spacing and significant increment can be noted in comparison with the corresponding single LSBs. The moment capacities of built-up LSBs were

compared with that of corresponding single LSBs and the comparisons are listed in Table 2. The beams, 200×45×1.6 LSB and 150×45×1.6 LSB, with connector spacing of span/6 had ultimate moments of 2.82 and 3.00 times the capacities of corresponding single LSBs, respectively. Thus the increment in moment capacity is about 40 – 50% for beams with AS/NZS 4600 recommended connector spacing of span/6, and is not negligible. However, the allowable capacity of back to back beams is typically determined by doubling the allowable capacity of single sections. This conservative assumption underestimates the true capacity of back to back LSB sections.

Table 2: Comparison of moment capacities

Test No	Specimens	s (mm)	M_{ub} (kNm)	M_{ub}/M_{us} ratio	Moment increment (%)
1	200×45×1.6 LSB	3500	17.15	2.34	17.0
2	200×45×1.6 LSB	1750	17.00	2.32	16.0
3	200×45×1.6 LSB	1167	21.06	2.87	43.5
4	200×45×1.6 LSB	875	17.93	2.45	22.5
5	200×45×1.6 LSB	583	20.64	2.82	41.0
6	150×45×1.6 LSB	3500	17.43	2.67	33.5
7	150×45×1.6 LSB	1750	17.28	2.65	32.5
8	150×45×1.6 LSB	1167	17.71	2.72	36.0
9	150×45×1.6 LSB	875	16.68	2.56	28.0
10	150×45×1.6 LSB	583	19.55	3.00	50.0

Note: M_{ub} – Ult. Moment of back to back LSB, M_{us} – Ult. Moment of singe LSB

The ultimate vertical deflection at midspan for built-up 200×45×1.6 LSB varied from 12.6 to 17.6 mm. For 150×45×1.6 LSB, the deflection varied from 30.8 to 35.1 mm while they were 55.8 and 54.4 mm for 125×45×2.0 LSB. The ultimate vertical deflection at midspan for single 200×45×1.6 LSB and 150×45×1.6 LSB are 13.0 and 39.3 mm, respectively and they are in or very close to the vertical deflection range of corresponding built-up LSB sections.

4.2 Failure mode

The failure mode was governed by lateral distortional buckling for all the back to back built-up specimens. The effect of cross-section distortion was governed by the depth of web. The slender section, 200×45×1.6 LSB, exhibited larger web distortion in comparison with other two sections (non-compact and compact sections). Also, the flange-web junction was distorted slightly. For 150×45×1.6

LSB, the web distortion was not as high as in the slender section. But flange rotation was very noticeable. Section 125×45×2.0 LSB exhibited very little web distortion and flange rotation. Single LSBs also exhibited lateral distortional buckling failure as shown by Mahaarachchi and Mahendran (2005a). The detrimental effects of lateral distortional buckling that occurs with single LSB sections appears to still remain with back to back LSBs, but it is not as severe as for single LSBs. Further numerical studies on both back to back and single LSB will investigate this. The deformation shape at failure for some selected built-up and single LSB specimens are shown in Figures 5 (a) and (b).

(a) (b)

Figure 5: Deformations at failure: (a) Back to back 150×45×1.6 LSB with CS of span/4 (b) Single 150×45×1.6 LSB

(a) (b) (c) (d)

Figure 6: Flange separation (a) 200×45×1.6 LSB with CS of span/2 (b) 150×45×1.6 LSB with CS of span/3 (c) 200×45×1.6 LSB with CS of span/6 (d) 150×45×1.6 LSB with CS of span/4

4.3 Flange separation and a review on current design rules

The second design rule is aimed at preventing excessive distortion between connectors by separation along the flange. Tests revealed different levels of separation between connectors, depending on connector spacing. Beams with connector spacings of span/4 and span/6 exhibited very little separation (≤ 1 mm) between the connectors located close to the supports (Figures 6c and d). Beams with connector spacings of span/2 and span/3 also showed smaller separations (≤ 3-4 mm) between the connectors (Figures 6a and b). Figures 6a to d show the level of separation, which is not significant from a design viewpoint.

Beams with connector spacing ratio of span/1 revealed sliding of webs on each other with a maximum value of about 5-6 mm, making the flanges not leveled. From the test results the limit of span/6 for connector spacing in AS 4600 (SA, 2005) appears to be over-conservative. In contrast, the limit given by BS 5950 Part 5 (BSI, 1998) of span/3 is an improvement. However, its second limit of not exceeding 50 times the minimum radius of gyration of the single beam makes the first limit irrelevant. For example, for all the tested specimens, the second limit is around 800 mm, which is less than the connector spacing of span/4 (875 mm). This makes the connector spacing of span/6 as the limit for the tested beams. The second rule governs the limit when the span length is increased. Hence using this second limit may also give overconservative results for long and intermediate span lengths. Thus, more suitable spacing limits are needed for the back to back LSBs with varying spans based on improved understanding.

5. Numerical Modelling of the Built-up LSB Section

5.1 General

In this research two finite element models, namely ideal and experimental models were developed using ABAQUS. Experimental models were generated to validate the finite element models in comparison with experimental results whereas ideal models were developed to conduct parametric studies and hence to develop design rules. The development of ideal models of built-up LSB beams is reported in Jeyaragan and Mahendran (2008b). The actual physical test system was simulated by experimental finite element model, which is described in the following sections.

5.2 Finite element mesh and material modelling

Based on convergence studies shell element, S4R5, was selected to model the LSB. This element is a thin, shear flexible, isometric quadrilateral shell with four nodes and five degree of freedom per node, utilizing reduced integration and bilinear interpolation scheme. Element widths ranging from 4.33 to 5.42 mm and a length

of 10 mm were selected as the suitable mesh size through the entire cross-section for both built-up and single LSB sections, which sufficiently represents the spread of plasticity, residual stress distribution and local buckling deformations. A simplified bi-linear stress-strain curve with no strain hardening, known as elastic-perfectly plastic model, was used in the experimental model for nonlinear analysis. This simple model was considered sufficient for modeling sections subject to a dominant failure mode of lateral buckling (Mahaarachchi and Mahendran, 2005b). Measured average yield stresses and thicknesses were adopted (Table 3).

Table 3: Measured average thicknesses and yield stresses

Section	Thickness (mm)			Yield stress (MPa)		
	t_o	t_i	t_w	f_{yo}	f_{yi}	f_{yw}
200x45x1.6 LSB	1.78	1.65	1.60	530	500	430
150x45x1.6 LSB	1.74	1.62	1.58	535	490	435

Note: t_o, t_i and t_w, and f_{yo}, f_{yi} and f_{yw} : Thicknesses and Yield stresses of outside flange, inside flange and web, respectively.

5.3 Load and boundary conditions

An idealized simply supported beam with a uniform moment within the span has generally been assumed as the worst scenario giving a lower bound solution. The following idealized simply supported (SS) boundary conditions were implemented in the ideal model:

1. SS in-plane: Both ends fixed against in-plane vertical deflection but unrestrained against in-plane rotation, and one end fixed against longitudinal horizontal displacement.
2. SS out-of-plane: Both ends fixed against out-of-plane horizontal deflection, and twist rotation, but unrestrained against minor axis rotation and warping displacements of flanges.

Simply supported boundary conditions implemented in the experimental models are slightly different from those in the ideal model and are described as follows:

1. The pin support end was modelled by restraining degree of freedom ‘234” for the node which controls the support plate as shown in Figure 7.
2. Due to the symmetry of beam, half span modelling was permitted by restraining degree of freedom “156” for all the nodes at mid span (Fig. 7).
3. Two point loads were applied on either side of the loading arm at the end of overhang (Figure 7).

The degree of freedom notations “1, 2 and 3” correspond to translation in x, y and z directions while “4, 5 and 6” represent the rotations about the x, y and z axes, respectively.

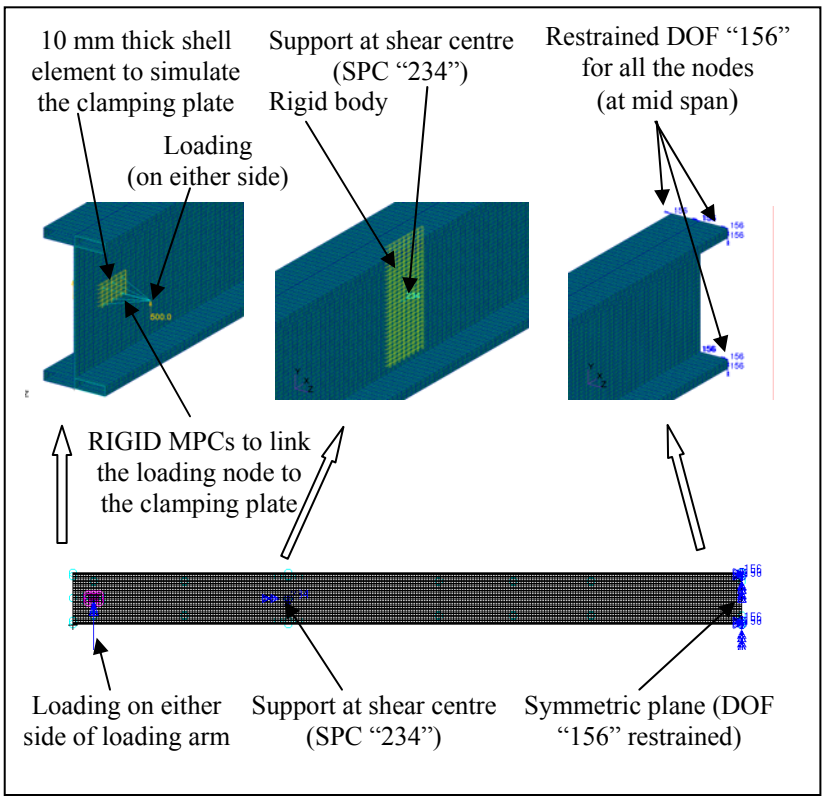

Figure 7: Load and boundary conditions for the experimental FE Model

The test members included rigid plates on either side of beam web at each support to prevent distortion and twisting of the cross-section. These stiffening plates were modelled as rigid body using R3D4 elements. The motion of the rigid body is controlled by a reference node. The control node was created at shear centre and support conditions ("234") were applied. In the experimental set-up, a concentrated load was applied at the end of each overhang, which was transferred equally to the two beam webs. Steel plates connected to the web were modelled using thicker shell element (10 mm) with elastic properties.

5.4 Fastener modelling

Fasteners play an important role in the structural response of built-up members. In this research, fasteners are designed with a greater factor of safety, and

therefore it is assumed that there will be no fastener failure. Beam element, B31, with a diameter of 10 mm, was used to model the fasteners. The material model for beam elements was elastic-perfectly plastic and a yield stress of 240 MPa was assumed. In the case of ideal model, perfect Tie MPC was simulated, which makes all active degrees of freedom equal on both sides of the connection.

5.5 Contact modelling

Contact modelling was implemented in order to simulate the interaction between the two LSB sections connected back to back. Surface-based contact simulation was found to be adequate to represent the contact interaction between them (Figure 8). Elements in the main web and the web of the flanges are likely to come into contact. Contact conditions were applied using symmetric "master-slave" algorithm, in which contact surface of one LSB was assigned as master surface while contact surface of other LSB was assigned as slave-surface. Small-sliding tracking approach, "hard" contact pressure-overclosure relationship, zero friction, deformable body conditions and initial gap of 0.1 mm were used in the element-based surface contact model.

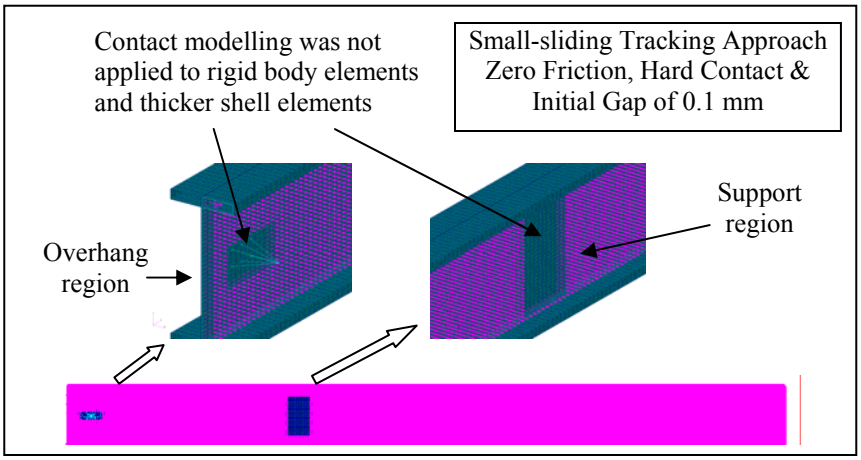

Figure 8: Contact modelling

5.6 Initial geometric imperfection

A geometric imperfection pattern is generally introduced for post buckling load-displacement analyses. The critical imperfection shape was introduced via ABAQUS *IMPERFECTION option by modifying the nodal coordinates using

a vector field created by scaling the lateral buckling eigenvector obtained from an elastic buckling analysis. Measured values were used in the models.

5.7 Residual stresses

The unique cold forming and dual electric resistance welding process of LSB sections introduces residual stresses, both flexural and membrane stresses. The residual stress model developed by Mahaarachchi and Mahendran (2005b) and upgraded by Seo et al. (2008) was used to introduce the initial stresses in the experimental models. The initial stresses were created using the SIGINI Fortran user subroutine and executed using ABAQUS *INITIAL CONDITIONS option, with TYPE = STRESS. The variation of the flexural residual stress through the thickness was assumed to be linear, with zero stress at the centre fibre. Nine integration points were defined through the thickness of each element to simulate the accurate distribution of residual stresses.

6. Calibration of Finite Element Models

It was necessary to validate the developed finite element models for numerical studies. For this purpose, elastic lateral buckling moments obtained using ideal finite element model were compared with the corresponding moments obtained from the established finite strip analysis program, THINWALL while the nonlinear analysis results from the experimental finite element model were compared with the experimental test results of LSBs.

6.1 Comparison of elastic lateral buckling moments

Elastic buckling moments obtained for the built-up LSB sections connected continuously were compared with the predictions from THIN-WALL (Table 4). The results agree well with an average deviation of (-) 5.5%. The numerical models used are not exactly identical since in the Thin-Wall model, separate elements were used to simulate the connections whereas in the ABAQUS finite element model, Tie MPCs were used at 10 mm intervals. This might have caused the observed differences.

6.2 Comparison with experimental test results

The nonlinear experimental finite element models were validated using the results from the experimental tests. Table 5 compares the ultimate moment capacity results of the nonlinear analyses using the experimental model described in Section 5 with the experimental test results. Typical bending moment versus deflection curves are provided in Figure 9.

Table 4: Comparison of elastic lateral buckling moments from finite element analysis (FEA) and Thin-Wall (TW)

Span (m)	Elastic Lateral Buckling Moment (kNm)								
	125×45×2.0 LSB			150×45×1.6 LSB			200×45×1.6 LSB		
	FEA	Thin-Wall	Dif (%)	FEA	Thin-Wall	Dif (%)	FEA	Thin-Wall	Dif (%)
2.00	40.91	43.23	5.4	31.60	33.10	4.5	32.95	34.66	4.9
3.00	28.74	30.45	5.6	22.57	23.69	4.7	22.36	23.52	4.9
4.00	22.12	23.46	5.7	17.73	18.63	4.8	17.45	18.39	5.1
5.00	17.94	19.04	5.8	14.57	15.33	5.0	14.37	15.15	5.1
6.00	15.07	16.00	5.8	12.34	12.99	5.0	12.21	12.88	5.2
7.00	12.98	13.78	5.8	10.69	11.25	5.0	10.60	11.19	5.3
8.00	11.40	12.00	5.8	9.42	9.92	5.0	9.35	9.88	5.3
9.00	10.15	10.78	5.8	8.42	8.86	5.1	8.37	8.84	5.3
10.00	9.15	9.72	5.8	7.60	8.01	5.1	7.57	7.99	5.3

Table 5: Comparison of nonlinear FEA and experimental results

Section	s (mm)	Type	Exp. results	FEA results	FEA/Exp.
200×45×1.6 LSB	1750	B	17.00	17.78	1.05
200×45×1.6 LSB	875	B	17.93	18.30	1.02
200×45×1.6 LSB	583	B	20.64	18.45	0.89
150×45×1.6 LSB	1750	B	17.28	16.43	0.95
150×45×1.6 LSB	1167	B	17.71	16.65	0.94
150×45×1.6 LSB	875	B	16.68	17.10	1.01
150×45×1.6 LSB	N/A	S	6.52	6.29	0.96
200×45×1.6 LSB	N/A	S	7.33	6.99	0.95

Note: Exp. – Experimental, FEA – Finite element analysis

Figures 10 (a) and (b) show the typical deformation of the test beams at failure and the corresponding failure predicted by FEA**.** Comparison of the ultimate moment capacities and the moment versus displacement curves of the tested specimens and the FEA shows a good agreement between tests and FEA.

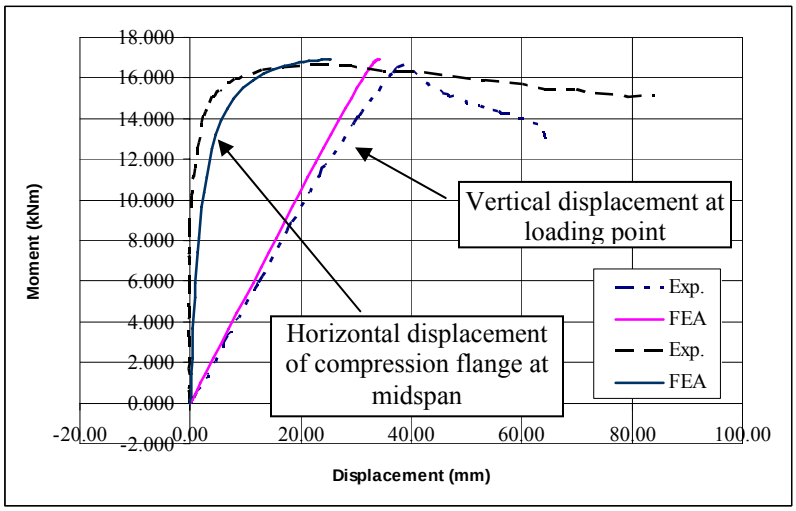

Figure 9: Moment versus displacement curve for back to back 150×45×1.6 LSB with connector spacing of span/4

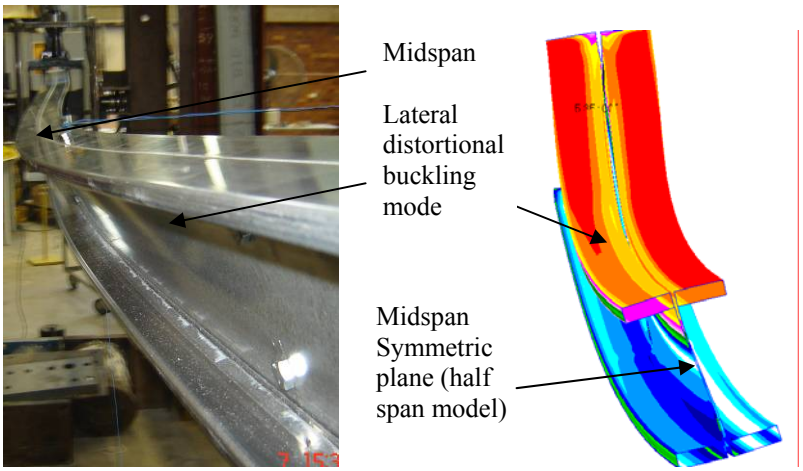

(a) Test - 150×45×1.6 LSB (b) FEA -150×45×1.6 LSB

Figure 10: Typical specimen deformation at failure (a) Tested specimen (b) Experimental finite element model

7. Elastic Buckling Moments and Applicability of Current Rules

Elastic buckling moments of a set of built-up LSB sections obtained from the ideal finite element models are listed in Table 6. Three different LSB sections, 125×45×2.0 LSB, 150×45×1.6 LSB and 200×45×1.6 LSB, were chosen from the small and medium size LSBs. Based on AS4100 guidelines, they are classified as compact, non-compact and slender sections, respectively. Intermediate span lengths (S) of 2, 3 and 4 m in which single LSB sections exhibit lateral distortional buckling were considered. In addition, connection spacing ratio (SR) of span/6 as specified in AS/NZS 4600, span/4, span/3, span/2, span/1 and continuous connections were considered. They are shown as "1, 2, 3, 4, 6, C" in Table 6.

Table 6: Elastic buckling moments in kNm from finite element analysis

S (m)	SR	125×45×2.0 LSB	150×45×1.6 LSB	200×45×1.6 LSB
2	1	28.82	22.99	22.80
	2	35.58	27.69	29.14
	3	37.09	28.76	30.11
	4	37.97	29.39	30.69
	6	38.89	30.06	31.32
	C	40.90	31.60	32.95
3	1	20.75	16.54	16.72
	2	25.35	20.12	20.17
	3	26.48	20.91	20.83
	4	27.06	21.32	21.19
	6	27.65	21.75	21.57
	C	28.74	22.57	22.36
4	1	16.11	13.18	15.64
	2	19.68	15.93	15.90
	3	20.56	16.56	16.41
	4	21.00	16.89	16.68
	6	21.42	17.19	16.95
	C	22.12	17.73	17.45

7.1 Design formulae for elastic buckling moment

Elastic buckling moment (M_o) is defined in Clause 5.6.1.1 of AS 4100 as follows:

$$M_o = \sqrt{\left[\left(\frac{\pi^2 EI_y}{L_e^2}\right)\left[GJ + \left(\frac{\pi^2 EI_w}{L_e^2}\right)\right]\right]} \quad (3)$$

Where E = Young's modulus, G = shear modulus, I_w = warping constant
I_y = second moment of area about the minor principal axis
J = torsion constant, L_e = effective length

Table 7: Comparison of elastic buckling moments obtained from Buckling formulae, Thin-wall and FEA

125×45×2.0 LSB							
L_e (m)	M_1	M_2	M_3	M_4	M_4/M_3	M_4/M_2	M_4/M_1
2.0	69.00	39.87	43.23	40.91	0.946	1.026	0.593
3.0	44.95	30.61	30.45	28.74	0.944	0.939	0.639
4.0	33.44	22.41	23.46	22.12	0.943	0.987	0.662
5.0	26.65	18.42	19.04	17.94	0.942	0.974	0.673
6.0	22.16	15.60	16.00	15.07	0.942	0.966	0.680
8.0	16.58	11.90	12.10	11.40	0.942	0.957	0.687
10.0	13.25	9.60	9.72	9.15	0.941	0.953	0.690
150×45×1.6 LSB							
L_e (m)	M_1	M_2	M_3	M_4	M_4/M_3	M_4/M_2	M_4/M_1
2.0	60.55	31.17	33.10	31.60	0.955	1.014	0.522
3.0	39.03	21.68	23.69	22.57	0.953	1.041	0.578
4.0	28.92	17.34	18.63	17.73	0.952	1.023	0.613
5.0	23.00	14.51	15.33	14.57	0.950	1.004	0.633
6.0	19.11	12.46	12.99	12.34	0.950	0.991	0.646
8.0	14.28	9.67	9.92	9.42	0.950	0.974	0.660
10.0	11.41	7.87	8.01	7.60	0.949	0.966	0.666
200×45×1.6 LSB							
L_e (m)	M_1	M_2	M_3	M_4	M_4/M_3	M_4/M_2	M_4/M_1
2.0	66.85	34.43	34.66	32.95	0.951	0.957	0.493
3.0	42.40	21.73	23.52	22.36	0.951	1.029	0.527
4.0	31.22	16.97	18.39	17.45	0.949	1.029	0.559
5.0	24.75	14.17	15.15	14.37	0.949	1.014	0.581
6.0	20.53	12.20	12.88	12.21	0.948	1.000	0.595
8.0	15.32	9.53	9.88	9.35	0.947	0.982	0.611
10.0	12.23	7.79	7.99	7.57	0.947	0.971	0.619

Note: M_1, M_2, M_3 and M_4 are Elastic buckling moment (M_o), Elastic lateral distortional buckling moment (M_{od}), and Elastic buckling moments obtained using thin-wall and FEA, respectively.

Pi and Trahair (1997) also provided equations to estimate the elastic distortional buckling moment (M_{od}) of hollow flange beam using an approximate effective torsional rigidity (GJ_e) as follows:

$$M_{od} = \sqrt{\frac{\pi^2 EI_y}{L^2}\left(GJ_e + \frac{\pi^2 EI_w}{L^2}\right)} \tag{4}$$

$$GJ_e = \frac{2GJ_F \dfrac{Et^3L^2}{0.91\pi^2 d}}{2GJ_F + \dfrac{Et^3L^2}{0.91\pi^2 d}} \tag{5}$$

Where, d = web height, L = length, t = thickness, J_e = effective torsion section constant, J_F = torsion constant of hollow flange

The beams with connector spacing of "C", continuous connection, is the upper bound for the back to back built-up LSBs with the particular fastener locations across the depth. The elastic buckling moments obtained from FEA, Thin-Wall and design formulae for beams with connector spacing of "C" were compared and listed in Table 7.

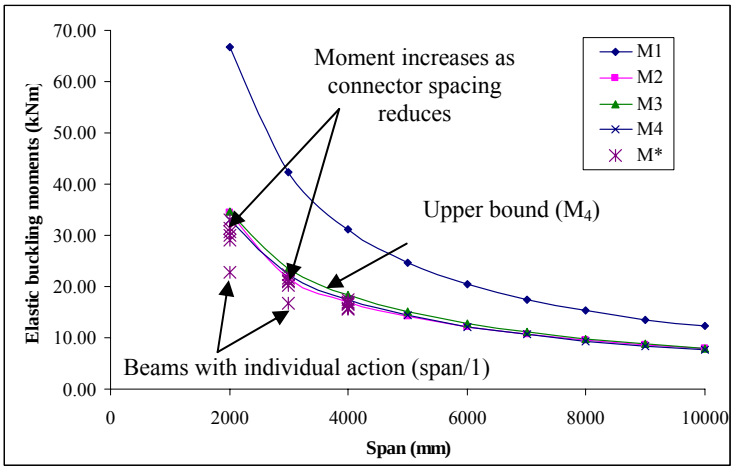

M* - Moment capacities of 200×45×1.6 LSBs with different fastener spacings

Figure 11: Comparison of elastic buckling moments for back to back 200×45×1.6 LSB

Elastic lateral distortional buckling moments obtained using Equation (4) agree well with FEA and Thin-wall results. But the elastic buckling moments obtained using Equation (3) did not agree with either FEA or Thin-wall. Figure 11 illustrates the comparison of elastic buckling moments for back to back 200×45×1.6 LSB section with different fastener spacings. It shows that the buckling formulae are unable to predict the elastic buckling moments of built-up LSBs as the connector spacing was increased.

8. Conclusion

This paper has described the details of an experimental study into the flexural behaviour of built-up LSB members, experimental finite element model development and the calibration of finite element models. Test results show that the built-up LSB sections are likely to give higher flexural capacities. The beams with a connector spacing of span/6 increased the flexural capacity by about 40 to 50% in comparison with the corresponding single LSBs. In the back to back built-up LSB sections even with larger connector spacings of span/2, the failure mode was governed by lateral distortional buckling with very little separation between the connectors. This shows that the current limit of span/6 specified in AS/NZS 4600 (SA, 2005) in relation to excessive deformation is over-conservative for intermediate spans. Thus, more appropriate spacing limits are needed for back to back LSBs with varying spans. Numerical models were developed and validated by comparing the elastic buckling moments and the nonlinear analysis results from numerical models with the results obtained from Thin-wall and experimental tests, respectively. The elastic lateral distortional buckling moments obtained for beams with connector spacing of "C", continuous connection, using Equation (4) agree well with the results from finite element analyses and Thin-wall. A detailed parametric study using the developed finite element model is currently under way to formulate improved design rules for built-up LSBs.

9. Acknowledgements

The authors would like to thank Australian Research Council and Australian Tube Mills for their financial support and the Queensland University of Technology for providing the necessary research facilities and technical support.

References

American Iron and Steel Institute (AISI) (2001). Specifications for the cold-formed steel structural members, Cold-formed Steel Design Manual, Washington, USA.

British Standards Institution (BSI) (1998). Structural use of steelwork in building, BS 5950, Part 5 Code of Practice for Design of Cold-formed Thin Gauge Sections, London, UK.

Jeyaragan, S. and Mahendran, M. (2008a). Experimental investigation of the new built-up LiteSteel beams, Proc. of the 5th International Conference on Thin-Walled Structures, Brisbane, Australia, (Paper accepted).

Jeyaragan, S. and Mahendran, M. (2008b). Numerical modeling and design of the new built-up LiteSteel beams, Proc. of the 5th International Conference on Coupled Instabilities in Metal Structures, Sydney, Australia, (Paper accepted).

Mahaarachchi, D. and Mahendran, M. (2005a). Lateral buckling tests of LiteSteel beam sections, Research Report, Queensland University of Technology, Brisbane, Australia.

Mahaarachchi, D. and Mahendran, M. (2005b), Finite Element Analysis of LiteSteel Beam Sections, Research Report, Queensland University of Technology, Brisbane, Australia.

Pi, Y.L. and Trahair, N.S. (1997), Lateral Distortional Buckling of Hollow Flange Beams, J. of Structural Engineering, ASCE, Vol. 123, No. 6, pp.695-702.

Seo, J.K., Anapayan, T. and Mahendran, M. (2008). Initial imperfection characteristics of mono-symmetric LiteSteel beams for numerical studies, Proc. of the 5th International Conference on Thin-Walled Structures, Brisbane, Australia, (Paper accepted).

Smorgon Steel LiteSteel Technologies (LST) (2005). Design capacity tables for LiteSteel beams, Smorgon Steel LiteSteel Technologies, Brisbane, Australia.

Standards Australia (SA) (1998), Steel Structures, AS 4100, Sydney, Australia.

Standards Australia (SA) (2005). Cold-formed steel structures, AS/NZS 4600, Sydney, Australia.